

---

# LieRE: Generalizing Rotary Position Encodings

---

Sophie Ostmeier\*  
sostm@stanford.edu

Brian Axelrod \*  
baxelrodresearch@gmail.com

Michael E. Moseley  
moseley@stanford.edu

Akshay Chaudhari†  
akshaysc@stanford.edu

Curtis Langlotz †  
langlotz@stanford.edu

## Abstract

While Rotary Position Embeddings (RoPE) for large language models have become widely adopted, their application for other modalities has been slower. Here, we introduce Lie group Relative position Encodings (LieRE) that goes beyond RoPE in supporting  $n$ -dimensional inputs. We evaluate the performance of LieRE on 2D and 3D image classification tasks and observe that LieRE leads to marked relative improvements in performance (up to 9.7% for 2D and up to 25.5% for 3D), training efficiency (3.5x reduction), data efficiency (30%) compared to the baselines of DeiT III, RoPE-Mixed and Vision-Llama. <https://github.com/Stanford-AIMI/LieRE>

## 1 Introduction

While the attention mechanism has achieved widespread use, especially as part of the transformer architecture, attention is invariant to the order of its inputs and requires another mechanism to capture positional information of input tokens [28]. This has spurred a line of work in the subarea of positional encodings—methods of encoding positional information in attention mechanisms.

In particular, Rotary Position Encoding (RoPE) has emerged as a technique for encoding relative positional information of text tokens in transformer-based models [23]. RoPE’s ability to capture relative position information has made it a popular choice for open-source language foundation models such as LLaMA. In particular, RoPE implicitly captures *relative* positions. When the token in position  $p_1$  attends to a token in position  $p_2$ , the effect of RoPE depends on  $p_1 - p_2$ .

Despite the success of RoPE in sequence tasks [26, 3], it is designed for one-dimensional sequence data. This has resulted in slow adoption for modalities with higher dimensional data, such as data that includes a temporal dimension like videos.

Our work aims to answer whether a single position encoding scheme can work well across both 2D and 3D modalities. If possible, this would enable the use of a simpler common model backbone across a variety of tasks.

### 1.1 Contributions

We introduce Lie Relative Encodings (LieRE), a mechanism that allows the attention mechanism to learn how to utilize relative spatial information of its inputs. We show that LieRE is effective on both 2D and 3D inputs of various modalities. Beyond improving classification accuracy, LieRE also reduces the amount of compute and data required during training to achieve a fixed accuracy. On the CIFAR100 task, this translates to 3.5x fewer training steps to achieve the same accuracy as the

---

\*equal contributions

†co-senior author

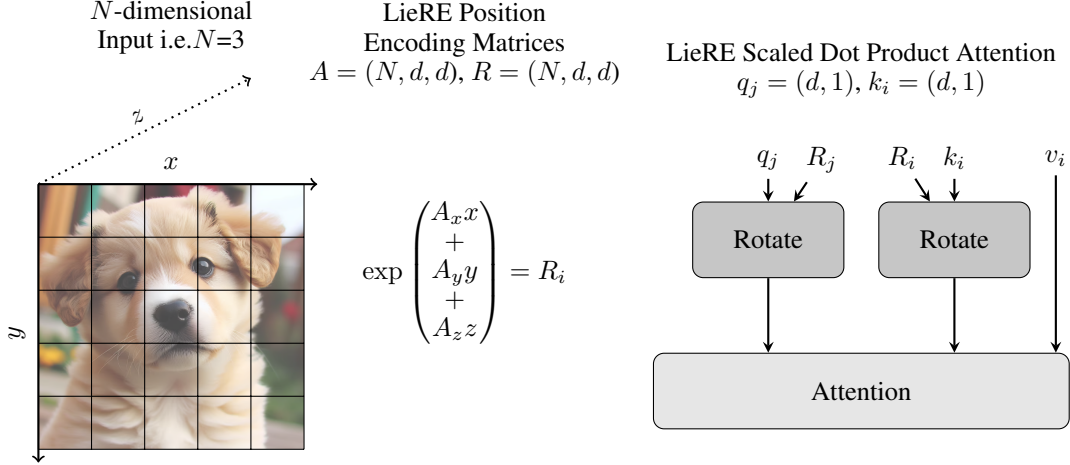


Figure 1: LieRE sketch, where  $A$  is a learnable skew symmetric matrix and  $R_i = \exp(A[x \ y \ z]) \in \mathbb{R}^{d \times d}$  is the rotation matrix for the first patch in the top left corner of the input with the position  $P_i = (x, y, z) \in \mathbb{R}^N$ .  $d$  is the head dimension. The upper triangle contains learnable  $\text{LieRE}_\theta$  parameter, while the lower triangle contains their negatives,  $-\text{LieRE}_\theta$ , reflecting the skew-symmetric nature of the matrix.

DeiT baseline and outperforming the DeiT baseline trained on the full set with only a 70% subset of the data. Furthermore, LieRE is simple to implement and adaptable to modalities, requiring only a tokenizer that also outputs a position in  $\mathbb{R}^d$  in addition to a standard embedding. In order to aid the reproducibility of our results we will post our code on github.

## 1.2 Related Work

### 1.2.1 Position Encodings

The fact that the original attention mechanism is invariant to the order of tokens has motivated the ongoing development of methods to incorporate positional information into the transformer architecture. We split our literature review into three broad classes of positional encodings: 1) absolute, 2) relative, and 3) contextual.

Absolute encodings generally operate on a per token-level, modifying the embedding of a token to encode the location of the token in the input. Methods such as sinusoidal and learned absolute encodings add vectors to the input token embedding [28, 7, 9]. Absolute position measures position with respect to an absolute reference, such as the start of the text or the top left corner of an image.

Relative position encodings instead encode the relative positions of two tokens. One strategy is to learn an embedding for position deltas which can be incorporated into the attention mechanism [20, 17, 16]. However, this incurs quadratic computational cost in terms of the number of tokens. Rotary Position Encodings (RoPE) avoid this cost by rotating the key and query vectors before the attention inner product. The algebraic properties of the block-diagonal rotation matrices used in RoPE ensures only relative positional information is captured in the attention mechanism [23]. RoPE is quite widely used in open source LLMs including the PaLM, Llama and Mixtral models [26, 3, 14]. However, RoPE can perform poorly on inference for larger context sizes than the model was trained on. This has spurred an active line of work extending RoPE to longer contexts, work which we review later.

We refer to the last category of positional as *contextual* position embeddings. This category is defined by encodings that aim to capture semantic positional information lost in traditional absolute and relative position encodings, often motivated by reasoning or mathematical tasks. Contextual Position encodings achieve (CoPE) this by allowing the model to learn how the position is computed [12]. Abacus embeddings enable transformers to learn how to handle arithmetic by better exposing the digit structure of numbers [18].

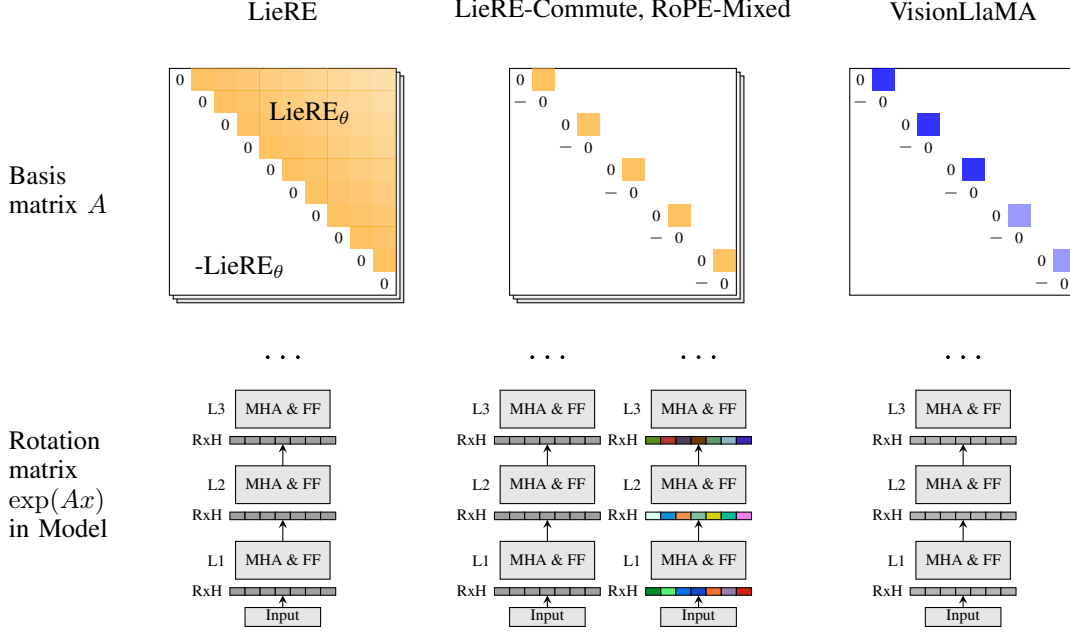


Figure 2: Comparisons of basis matrix  $A$  of our work, Rope-Mixed [13], VisionLlama [4]. First row: learnable parameter (yellow), not learnable parameter (blue) in basis matrix. Second row: rotation matrices  $\exp(Ax)$  shared across the stem (gray) or different for each layer and head (colorful). MHA := Multi-Head-Attention, FF := Feed Forward, L[index] := Layer index, RxH := Rotation Matrix per Head,  $\text{LieRE}_\theta$  := the number of LieRE parameters.

### 1.2.2 Extensions of RoPE

The efficiency and popularity of RoPE have led to several lines of work looking to extend it focused on specific domains.

One notable one is context extension, which aims to address the fact that RoPE NLP models trained on short documents tend to perform poorly on long documents. Methods like NTK-aware context extension, YaRN and LongRoPE focus on enabling already trained models to handle long context, both with and without finetuning [8, 19, 27, 2].

Another line of work has been specifically focused on adapting RoPE to image tasks. Both VisionLlama and RoPE-Mixed present relative position encodings inspired by RoPE that are able to encode 2D positional data [4, 13]. The primary difference is that RoPE-Mixed has a learnable component, whereas VisionLlama does not.

## 2 Background

### 2.1 Lie Groups in the Context of Attention

In this section, we aim to provide a minimal introduction to Lie groups so that the reader is able to understand the mathematical motivations behind LieRE. Lie groups are well studied, especially in the context of representation theory, and standard texts including [11] are able to provide a more extensive introduction to the subject.

In this context, Lie groups are smooth sets of matrices that are closed under matrix multiplication and inversion. For every Lie group, the matrix exponential provides a smooth bijective map from a subset of  $\mathbb{R}^{n \times n}$  (hereto referred to as the generator set) to the Lie group. The exponential map is a diffeomorphism and has the following key property for generators  $U, V \in \mathbb{R}^{n \times n}$  close together:

$$\exp(U - V) = \exp(-V + U) \approx \exp(V)^{-1} \exp(U) \quad (1)$$

Section 3.1 will show that this is the key to being able to encode relative positions.

Both RoPE (in the context of text) and RoPE-Mixed use block-diagonal rotation matrices with 2D rotations as blocks. These form a special Lie group that is commutative, allowing us to strengthen the statement in equation (1) to

$$\exp(U - V) = \exp(U) \exp(V)^{-1} = \exp(U)^{-1} \exp(V). \quad (2)$$

Our work examines the tradeoff between using the stronger property in equation (2) or increased capacity and the weaker property (1).

### 3 Methods

#### 3.1 Rotations for Relative Positions in Attention

Before introducing the pseudocode we explain how LieRE modifies the attention mechanism and how this relates to Lie groups.

We start by using a learnable linear map to embed the positions as skew-symmetric matrices  $P_i$  and  $P_j$  and compute high dimensional rotations as  $R_i = \exp(P_i)$  and  $R_j = \exp(P_j)$ . Learning in the space of skew symmetric matrices allows us to sidestep some of the difficulty that would come from learning on the manifold of rotation matrices.

Recall that, for every pair of tokens, the attention mechanism computes the inner products between their key and query vectors,  $k_i^T q_j$ , as shown in figure 1. We encode the positions by multiplying by the rotation matrices in the prior part. In particular, we update the keys and queries as  $k'_i = k_i R_i$  and  $q_j = q_j R_j$ . This results in an updated inner product of  $(R_i k_i)^T R_j q_j = k_i R_i^T R_j q_j = k_i R_i^{-1} R_j q_j$ .

Recall that by equation 1,  $R_i^{-1} R_j = \exp(P_i)^{-1} \exp(P_j) \approx \exp(P_j - P_i)$ . In other words, the inner product automatically computes the relative position encoding. Note that this is the mechanism behind the original RoPE paper. The difference is that LieRE uses the full set of high dimensional rotations and relaxes the constraint that equation 1 holds with equality. We make the description of the method more precise in the next section.

#### 3.2 LieRE

LieRE modifies the attention mechanism by applying a rotation to the keys and queries before computing their inner products. However, where RoPE applies a block-diagonal rotation matrix with 2D rotation matrices as blocks, LieRE applies a  $n \times n$  rotation matrix (Figure 1). Using the fact that every rotation matrix can be represented as the matrix exponential of a skew-symmetric matrix, we parametrize the rotations with generators before the matrix exponential. This skew-symmetric generator is computed via a learned linear map from the positions to the generator space. Let  $x \in \mathbb{R}^n$  indicate the position of the token, and  $A : \mathbb{R}^d \rightarrow \text{Skew}_n(\mathbb{R})$  be a learnable linear map to the set of skew-symmetric matrices. At the start of every forward pass, we compute the LieRE rotation matrix for each token as

$$R_{\text{LieRE}} := \exp(Ax).$$

Then, for each attention mechanism, the keys and queries for a particular token are updated as  $\text{key}' := R_{\text{LieRE}} \cdot \text{key}$ ,  $\text{query}' := R_{\text{LieRE}} \cdot \text{query}$ . We present attention with LieRE and LieRE-Commute side by side in algorithms 1 and 2.

Outside of the generator scaling experiments, we set the rotation dimension equal to the head dimension and apply rotation on a per-attention-head basis.

Note that if we apply sparsity structure that enforces 2x2 blocks we recover commutativity. We refer to this configuration and LieRE-Commute. If we then have separate learnable parameters for every layer and head, we recover RoPE-mixed [13].

---

**Algorithm 1** RoPE Attention (prior work for text), rot=rotated

---

```

1: procedure ROPE( $X, p, d$ )
2:    $\theta \leftarrow \frac{1}{10000^{2i/d}} \quad \forall i \in [0, d)$ 
3:   for  $i \leftarrow 0$  to  $d$  step 2 do
4:      $X_{\text{rot}}^i \leftarrow X^i \cos p\theta^i - X^{i+1} \sin p\theta^i$ 
5:      $X_{\text{rot}}^{i+1} \leftarrow X^i \sin p\theta^i + X^{i+1} \cos p\theta^i$ 
6:   end for
7:   return  $X_{\text{rotated}}$ 
8: end procedure

9: procedure ROPEATTENTION( $Q, K, V$ )
10:   $p \leftarrow \text{tokenPositions}$ 
11:   $d \leftarrow \text{embeddingDimension}$ 
12:   $K_{\text{rot}} \leftarrow \text{ROPE}(K, p, d)$ 
13:   $Q_{\text{rot}} \leftarrow \text{ROPE}(Q, p, d)$ 
14:   $\text{Attention} \leftarrow \text{softmax} \left( \frac{Q_{\text{rot}} K_{\text{rot}}^T}{\sqrt{d}} \right) V$ 
15:  return Attention
16: end procedure

```

---



---

**Algorithm 2** LieRE Attention (our work), rot=rotated

---

```

1: procedure LIERE( $X, p, A$ )
2:   rotation_matrix  $\leftarrow \exp(Ap)$ 
3:    $X_{\text{rot}} \leftarrow X \odot \text{rotation\_matrix}$ 
4:   return  $X_{\text{rot}}$ 
5: end procedure

6: procedure LIEREATTENTION( $Q, K, V, A$ )
7:    $p \leftarrow \text{tokenPositions}$ 
8:    $K_{\text{rot}} \leftarrow \text{LIERE}(K, p, A)$ 
9:    $Q_{\text{rot}} \leftarrow \text{LIERE}(Q, p, A)$ 
10:   $\text{Attention} \leftarrow \text{softmax} \left( \frac{Q_{\text{rot}} K_{\text{rot}}^T}{\sqrt{\dim(K)}} \right) V$ 
11:  return Attention
12: end procedure

```

---

## 4 Experiments

### 4.1 Model and Training Parameters

In order to isolate the effect of changing the position encoding, we use a standard<sup>3</sup> transformer backbone modified to be able to switch between relative position encoding types. We use the standard backbone sizes of ViT-Tiny, ViT-B and ViT-L [9]. All experiments use RandAugment [5]. We avoid using pre-trained weights in order to maximize the comparability of results between methods. In order to ensure a fair comparison, we explicitly avoid tuning hyperparameters with LieRE and use the same default hyperparameters for all experiments (Appendix B).

### 4.2 Datasets and Tasks

Our experiments are designed to evaluate the efficacy of LieRE as a position encoding across both 2D and 3D data. We evaluate LieRE on the classification of 2D (images) and 3D (videos) data. For 3D data and ImageNet-1k (2D), we focus on accuracy. For CIFAR-100 (2D), where training is less resource intensive, we also evaluate LieRE’s data and training compute efficiency.

#### 4.2.1 2D Classification

For 2D data we evaluate performance on the CIFAR-100 and ImageNet-1k image classification task [15, 6]. We partition our evaluation of performance into four parts. In the first part, we examine accuracy across a range of model architectures on both CIFAR-100 and ImageNet-1k and compare to absolute [9] position encoding and recent related work, RoPE-Mixed [13], VisionLlama embeddings [4].

In the second part, we take advantage of the relatively modest amount of compute resources necessary to train a model for CIFAR-100 to examine LieREs impact on data efficiency. We also measure training *compute* efficiency by comparing the number of training steps necessary to achieve a fixed level of validation accuracy.

In the third part, we evaluate the impact of LieRE with various scales. We vary the capacity of the transformer backbone with corresponding to ViT-T, ViT-B and ViT-L, as proposed in [9], the number of learned LieRE generators (one, per-attention-head and per-layer) and the LieRE generator capacity by imposing a block diagonal structure on the generator that allows us to vary the added capacity.

---

<sup>3</sup><https://github.com/kentaroy47/vision-transformers-cifar10>

Table 1: 2D image and 3D video classification Top-1 Accuracy (95% confidence intervals) results. All models use 85.1M parameters for 2D tasks and 88.7M parameters for 3D task [15, 6, 21, 22] \* equivalent to DeiT, \*\* equivalent to Vivit (spatio-temporal).

Method	CIFAR-100	ImageNet-1k	UCF101
Abs. Pos. E. *,**	63.9 (62.9-65.8)	66.1 (65.7-66.5)	42.7 (42.3-43.1)
VisionLlama RoPE	65.5 (64.6-66.5)	65.4 (65.0-65.8)	50.5 (50.1-50.9)
RoPE-Mixed	63.7 (61.8-65.6)	65.9 (65.5-66.3)	45.7 (45.2-46.0)
LieRE-Commute	66.9 (66.0 - 67.9)	68.4 (67.9-68.9)	52.1 (51.7-52.5)
LieRE	<b>69.9 (68.9-70.8)</b>	<b>69.5 (69.1-69.9)</b>	<b>53.6 (53.2-54.0)</b>

In the fourth part, we measure how much different models depend on the positional information in the image/video by shuffling the patches. A higher accuracy drop with randomly shuffled patches means the model relies more on the positions of the patches during inference.

#### 4.2.2 3D Classification

In this section, we introduce Rotary Position Encodings for 3D data and compare LieRE-based transformers with transformers with RoPE-mixed and absolute encoding similar to the previous section [1, 13]. For the 3D experiments, we examine video classification performance in the UCF101 dataset [21]. Again, we did not optimize any hyperparameters for the LieRE model and used the dataloader from [24]. The full set of hyperparameters may be found in appendix B.

## 5 Results

### 5.1 Accuracy

For 2D images, we show that the LieRE-based transformer outperforms the DeiT by a relative performance improvement of 9.4% [25], RoPE adaptation in VisionLlama [4] by 6.7% and RoPE-Mixed by 9.7% on CIFAR-100 [13].

For 3D inputs (video), we observe an relative accuracy improvement of LieRE-based transformer over the absolute position embedding of up to 25.5 % and RoPE-inspired position encodings at least to 6.1% in accuracy.

### 5.2 Data efficiency

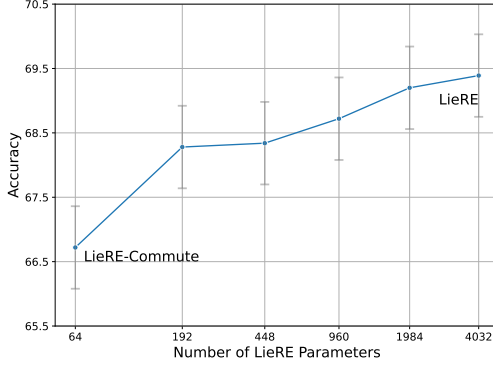
We observe that transformers based on LieRE exhibit greater data efficiency compared to leading transformer architectures for 2D images on the CIFAR-100 dataset. For instance, when using 40% of the dataset, the LieRE-based transformer outperforms all comparable methods by 4.5 percentage points. Additionally, there is a mild trend indicating that the performance gap widens as the amount of data decreases (Figure 3b).

### 5.3 Model Scaling

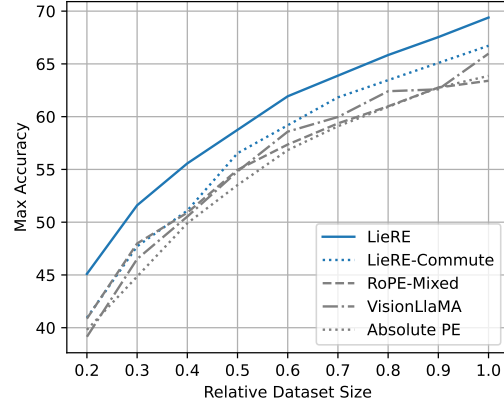
We examine three axes of capacity scaling: transformer backbone parameters, LieRE generator parameters and learning separate LieRE generators across heads and layers. Here we find a surprising result that RoPE-mixed can be substantially improved by sharing parameters across attention heads and layers and not learning them separately.

#### 5.3.1 Transformer backbone capacity

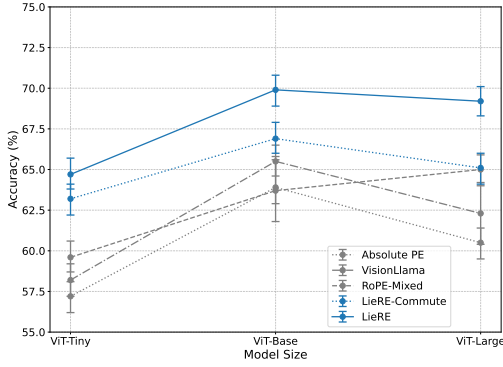
We also evaluate how the inclusion of LieRE affects performance across model sizes on the CIFAR-100 in Figure 4a. We observe that LieRE retains a statistically significant lead in performance across all three model sizes.



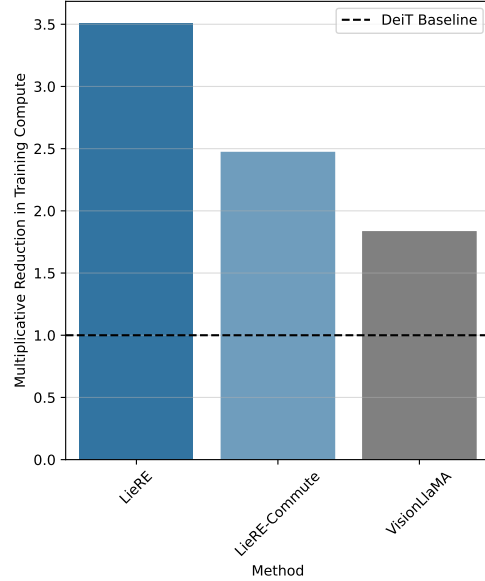
(a) Performance scales with generator dimension the number of LieRE parameters, compared to LieRE with one skew-symmetric matrix learned for the entire model (stem).



(b) Data ablation on for different position embeddings on CIFAR-100.



(a) Performance behavior on CIFAR-100 (2D Image Classification) over ViT-Tiny (22M), ViT-Base (85M), ViT-Large (302M) for LieRE Rope-Mixed and Absolute Encoding (Appendix, table 5).



(b) The LieRE spatial encoding allows the model to match the performance of absolute position encodings with substantially less training time.

### 5.3.2 Generator parameters

LieRE adds a small amount of capacity to the model (4032 parameters for the ViT-B backbone we use for most experiments), leading to the natural question of how helpful the marginal capacity is.

We vary capacity by enforcing a block diagonal structure on the generator. Varying the block size allows us to approach "full" LieRE. Recall that using  $2 \times 2$  blocks recovers exact commutativity and is referred to as LieRE-commute. This configuration substantially outperforms RoPE-Mixed, despite differing only in that it uses the same parameters across heads and layers and RoPE-Mixed learns separate parameters.

In figure 3a we evaluate accuracy versus block dimension. We observe the steepest increase at the very start, though accuracy continues to grow as the generator dimension increases.



Table 2: Layer, Head and Stem Learnable Rotary Embeddings on CIFAR-100, ViT-B, \* equivalent to LieRE-Commute

FLOP	Stem	Heads	Layers	Rope-Mixed	LieRE	Reference
5.684G		✓	✓	63.0	64.5	[13]
5.684G		✓		63.6	65.1	
5.613G			✓	<b>68.3</b>	69.9	
5.613G	✓			66.9*	<b>69.9</b>	(ours)

### 5.3.3 Sharing LieRE Parameters Across Heads and Layers

We also examine whether learning separate positional encoding per attention head and per layer improves performance on CIFAR-100 in table 2. We conduct this experiment for both RoPE-Mixed and LieRE and observe that in both cases it is best to learn one set of parameters across heads and layers. This is the mechanism by which we are able to show larger improvements from adopting RoPE-Mixed than the original paper [13]. We name this transformed form of RoPE-Mixed LieRE-Commute, since it is equivalent to LieRE with generator dimension 2 (see Figure ??).

## 5.4 Compute efficiency

Training transformers can necessitate substantial computational resources, which can hinder equitable access to research and development of machine learning methods. We demonstrate that the LieRE-based transformer requires 3.5 times less training epochs on Cifar100 to achieve comparable performance to the Absolute Position Embedding baseline (as used in DeiT III [25]). This represents the largest reduction in training time compared to recent works such as VisionLlama and RoPE-Mixed [4, 13]. We note that this is the first training efficiency comparison of these recent methods. Figure 4b shows the amount of allowable compute reduction to achieve the same accuracy achieved by absolute position encodings (DeiT baseline) after 200 epochs. LieRE demonstrates the largest win, allowing a 3.5X reduction in training compute to achieve the same accuracy.

## 5.5 FLOP analysis

We find that since all methods we examine introduce a computational cost that is at most linear in the number of tokens, and runtime is dominated by the quadratic attention component, there is no substantial difference in computational efficiency between the methods. We list inference FLOP of the various methods in table 3.

Table 3: FLOP analysis with percentage increase compared to absolute position encodings

Position Enc.	ViT-Tiny (22M)	ViT-Base (85M)	ViT-Large (302M)
Abs. Pos. E.*	0.963G	5.607G	19.856G
VisionLlaMA RoPE	0.963G (+0.001%)	5.607G (+0.002%)	19.856G (+0.000%)
RoPE-Mixed	0.963G (+0.001%)	5.609G (+0.036%)	19.863G (+0.035%)
LieRE-Commute (ours)	0.963G (+0.000%)	5.608G (+0.018%)	19.858G (+0.005%)
LieRE (ours)	0.970G (+0.727%)	5.613G (+0.107%)	19.869G (+0.065%)

## 5.6 Patch shuffling

Shuffling patches and frames allows us to see how much the model is able to use the positional information in its inputs. A model whose architecture does not allow/encourage the use of positional information will converge to a representation similar in spirit to a bag-of-words, where the relative locations of pixels/voxels do not matter. A greater dropoff in accuracy during shuffling is indicative that the model more heavily utilizes positional information.

We evaluate models using the decline in accuracy when evaluating on shuffled patches. We observe the most significant decline LieRE-based transformers, leading to the conclusion that LieRE models



Table 4: Relative accuracy drop for 2D image classification (CIFAR-100) and Video recognition (UCF101) after patch shuffling

Method	CIFAR-100 (2D)			UCF101 (3D)		
	Before Shuffling↑	After Shuffling↓	Drop(%)↑	Before Shuffling↑	After Shuffling↓	Drop(%)↑
Abs. Pos. E.	63.9	19.6	69.3	42.7	42.5	0.0
VisionLlama RoPE	65.8	29.7	54.8	50.5	36.2	28.5
RoPE-Mixed	63.6	38.7	39.0	45.7	37.9	17.1
LieRE-Commute	66.9	16.5	75.4	52.1	37.2	28.6
LieRE	69.9	15.9	<b>77.1</b>	53.6	24.7	<b>53.9</b>

are most capable at using positional information. The complete results are displayed for CIFAR-100 and table for UCF101 (Table 4) .

## 6 Limitations

While LieRE shows promising results across multiple modalities and input dimensionalities, there are a few limitations worth noting. Our method is specifically designed to modify the inner product, making it compatible with most attention schemes, including original attention and linear attention. However, this specificity may limit its applicability to other architectures, like convolutional neural networks, that do not rely on inner product-based attention mechanisms. Future work could explore adaptations of our method to a wider range of architectures. Furthermore, the current formulation of our method is designed to encode vector positions in  $\mathbb{R}^d$ . While this is sufficient for many applications, it may not be directly applicable to tasks that require encoding poses in  $SE(3)$  like robotics. Further research may be necessary to adapt our method to effectively handle such representational requirements.

Despite these limitations, we believe that our work provides much-needed insight into how to improve model performance and reduce training costs by encoding relative position information across various modalities and input dimensionalities.

## 7 Broader Impacts

LieRE, our proposed method for encoding positional information in attention mechanisms, has demonstrated improvements in 2D image and video classification tasks. We are particularly excited about how LieRE can expand the applicability transformers to  $n$  dimensional inputs. This may lay down the tracks to apply that same relative position encoding within and across modalities and settings.

## 8 Conclusion

In this paper, we introduced Lie group Relative position Encodings (LieRE), a position encoding that can effectively encode relative position information for attention mechanisms across modalities and input dimensionalities. Through experiments on 2D image classification (CIFAR-100, ImageNet-1k) and 3D video classification (UCF101), we demonstrated that LieRE achieves better performance compared to existing positional encoding methods. Beyond improving accuracy, LieRE also exhibits data and compute efficiency. On CIFAR-100, LieRE requires 3.5 times less training computed to match the performance of the baseline model with absolute position encodings. Furthermore, LieRE can outperform the baseline trained on the full dataset while using only 70% of the training data, highlighting its data efficiency. The key advantages of LieRE include its simplicity, flexibility, and ease of adaptation to new modalities. By requiring no changes to the tokenizer other than outputting positions and no other code changes, LieRE may provide a unified and efficient approach for transformers to process and learn from various data modalities within a single architecture.

## References

- [1] Anurag Arnab et al. “Vivit: A video vision transformer”. In: *Proceedings of the IEEE/CVF international conference on computer vision*. 2021, pp. 6836–6846.
- [2] Shouyuan Chen et al. “Extending context window of large language models via positional interpolation”. In: *arXiv preprint arXiv:2306.15595* (2023).
- [3] Aakanksha Chowdhery et al. “Palm: Scaling language modeling with pathways”. In: *Journal of Machine Learning Research* 24.240 (2023), pp. 1–113.
- [4] Xiangxiang Chu et al. “VisionLLaMA: A Unified LLaMA Interface for Vision Tasks”. In: *arXiv preprint arXiv:2403.00522* (2024).
- [5] Ekin D Cubuk et al. “Randaugment: Practical automated data augmentation with a reduced search space”. In: *Proceedings of the IEEE/CVF conference on computer vision and pattern recognition workshops*. 2020, pp. 702–703.
- [6] Jia Deng et al. “Imagenet: A large-scale hierarchical image database”. In: *2009 IEEE conference on computer vision and pattern recognition*. Ieee. 2009, pp. 248–255.
- [7] Jacob Devlin et al. “BERT: Pre-training of Deep Bidirectional Transformers for Language Understanding”. In: *Proceedings of the 2019 Conference of the North American Chapter of the Association for Computational Linguistics: Human Language Technologies, Volume 1 (Long and Short Papers)*. 2019, pp. 4171–4186.
- [8] Yiran Ding et al. “LongRoPE: Extending LLM Context Window Beyond 2 Million Tokens”. In: (2024). arXiv: [2402.13753 \[cs.CL\]](https://arxiv.org/abs/2402.13753).
- [9] Alexey Dosovitskiy et al. “An image is worth 16x16 words: Transformers for image recognition at scale”. In: *arXiv preprint arXiv:2010.11929* (2020).
- [10] William A Falcon. “Pytorch lightning”. In: *GitHub* 3 (2019).
- [11] William Fulton and Joe Harris. *Representation theory: a first course*. Vol. 129. Springer Science & Business Media, 2013.
- [12] Olga Golovneva et al. “Contextual Position Encoding: Learning to Count What’s Important”. In: *arXiv preprint arXiv:2405.18719* (2024).
- [13] Byeongho Heo et al. “Rotary Position Embedding for Vision Transformer”. In: *arXiv preprint arXiv:2403.13298* (2024).
- [14] Albert Q Jiang et al. “Mixtral of experts”. In: *arXiv preprint arXiv:2401.04088* (2024).
- [15] Alex Krizhevsky, Geoffrey Hinton, et al. “Learning multiple layers of features from tiny images”. In: (2009).
- [16] Ze Liu et al. “Swin transformer v2: Scaling up capacity and resolution”. In: *Proceedings of the IEEE/CVF conference on computer vision and pattern recognition*. 2022, pp. 12009–12019.
- [17] Ze Liu et al. “Swin transformer: Hierarchical vision transformer using shifted windows”. In: *Proceedings of the IEEE/CVF international conference on computer vision*. 2021, pp. 10012–10022.
- [18] Sean McLeish et al. “Transformers Can Do Arithmetic with the Right Embeddings”. In: *arXiv preprint arXiv:2405.17399* (2024).
- [19] Bowen Peng et al. “Yarn: Efficient context window extension of large language models”. In: *arXiv preprint arXiv:2309.00071* (2023).
- [20] Peter Shaw, Jakob Uszkoreit, and Ashish Vaswani. “Self-attention with relative position representations”. In: *arXiv preprint arXiv:1803.02155* (2018).
- [21] Khurram Soomro, Amir Roshan Zamir, and Mubarak Shah. “UCF101: A dataset of 101 human actions classes from videos in the wild”. In: *arXiv preprint arXiv:1212.0402* (2012).
- [22] Anouk Stein et al. “RSNA Intracranial Hemorrhage Detection”. In: (2019). URL: <https://kaggle.com/competitions/rsna-intracranial-hemorrhage-detection>.
- [23] Jianlin Su et al. “RoFormer: Enhanced transformer with Rotary Position Embedding”. In: *Neurocomputing* 568 (2024), p. 127063. ISSN: 0925-2312. DOI: <https://doi.org/10.1016/j.neucom.2023.127063>. URL: <https://www.sciencedirect.com/science/article/pii/S0925231223011864>.
- [24] Zhan Tong et al. “Videomae: Masked autoencoders are data-efficient learners for self-supervised video pre-training”. In: *Advances in neural information processing systems* 35 (2022), pp. 10078–10093.

- [25] Hugo Touvron, Matthieu Cord, and Hervé Jégou. “Deit iii: Revenge of the vit”. In: *European conference on computer vision*. Springer. 2022, pp. 516–533.
- [26] Hugo Touvron et al. “Llama: Open and efficient foundation language models”. In: *arXiv preprint arXiv:2302.13971* (2023).
- [27] Szymon Tworkowski et al. “Focused transformer: Contrastive training for context scaling”. In: *Advances in Neural Information Processing Systems* 36 (2024).
- [28] Ashish Vaswani et al. “Attention is all you need”. In: *Advances in neural information processing systems* 30 (2017).

## A Appendix

### B Experiment Hyperparameters

The backbone for all experiments is configured as ViT-B, with 12 layers, a hidden dimension of 768, and an intermediate dimension of 3096. We use a dropout of 0.1. We used CLS pooling in our implementation to facilitate comparability with existing literature in the field. Further experiments revealed substantial performance improvement with mean pooling and LieRE. We use the pytorch lightning framework for all experiments [10].

#### B.1 2D Image Classification

The CIFAR experiments were trained on 8xL4 GPUs with 24GB of VRAM each and all took under 30 minutes to complete. The generator scaling experiment was conducted using RTX6000 GPUs. The ImageNet experiments were trained on 8xL40 GPUs and all took less than 2 days and 5 hours of runtime including time lost due to preemption and resource sharing. We use a cosine learning rate schedule with an initial learning rate of  $1E-4$  and train for 200 epochs. We use an effective batch size of 512. We use a patch size of  $4 \times 4$  on the original  $32 \times 32$  image for CIFAR-100 and a patch size of  $16 \times 16$  on the randomly cropped and resized  $224 \times 224$  image. All vision experiments used RandAugment [5]. We use the ADAM optimizer with betas of 0.9 and 0.999 and  $\epsilon = 1e-8$ . The hyperparameters were tuned with RoPE-mixed and selected before conducting the LieRE trainers as to ensure a fair comparison.

#### B.2 3D Video Classifications

The 3D classification experiments were conducted on either  $8 \times A100$  40GB GPUs or  $4 \times A100$  80GB GPUs with the effective batch size held constant either by using a gradient accumulation or increasing the batch size. Similar to 2D classification, we use an initial learning rate of  $1E-4$  with a cosine decay, trained for 200 epochs, and had a total batch size of 64 and a patch size of  $2 \times 16 \times 16$  on the randomly cropped and resized  $32 \times 224 \times 224$  video/image. We use the ADAM optimizer with betas of 0.9 and 0.999 and  $\epsilon = 1e-8$ .

#### B.3 Scaling Model Size

Table 5: Comparison of Position Encoding Methods for Different ViT Models, Accuracy (bootstrapped 95%CI)

Position Encoding	ViT-Tiny	ViT-Base	ViT-Large
Abs. Pos. E.	57.2 (56.2 - 58.1)	63.9 (62.9 - 65.8)	60.5 (59.5 - 61.4)
VisionLlaMA RoPE	58.2 (57.2 - 59.2)	65.5 (64.6 - 66.5)	62.3 (60.4 - 64.2)
RoPE-Mixed	59.6 (58.7 - 60.6)	63.7 (61.8 - 65.6)	65.0 (64.0 - 65.9)
LieRE-Commute	63.2 (62.2 - 64.1)	66.9 (66.0 - 67.9)	65.1 (64.1 - 66.0)
LieRE	64.7 (63.8 - 65.7)	69.9 (68.9 - 70.8)	69.2 (68.3 - 70.1)

#### B.4 Python implementation of skew-symmetric matrix

---

```

1 generator_raw_params = nn.Parameter(
2     torch.rand(
3         input_dimensionality,
4         head_dim,
5         head_dim,
6     ) * 2 * math.pi # optional, inspired from RoPE-Mixed paper
7 )
8
9 upper_triangle = (
10     torch.triu(generator_raw_params, diagonal=1)
11 )
12 skew_bases = upper_triangle - torch.transpose(upper_triangle, -1, -2)
13 in_basis_positions = (
14     positions.reshape(list(positions.shape) + [1] * 2) * skew_bases
15 )
16 generator_pos = torch.sum(in_basis_positions, dim=-3)
17 rotation = torch.matrix_exp(generator_pos.to(dtype=torch.float32)).to(
18     dtype=positions.dtype)

```

---